DEUTSCHES ELEKTRONEN-SYNCHROTRON DESY

DESY 88-104
July 1988

SENSITIVITY OF W' AND Z' SEARCHES AT HERA

by

F. Cornet

MPI f. Physik u. Astrophysik, WHI f. Physik, München

R. Rückl

Deutsches Elektronen-Synchrotron DESY, Hamburg

ISSN 0418-9833

NOTKESTRASSE 85 · 2 HAMBURG 52

To be sure that your preprints are promptly included in the
HIGH ENERGY PHYSICS INDEX ,
send them to the following address (if possible by air mail) :

DESY
Bibliothek
Notkestrasse 85
2 Hamburg 52
Germany

DESY 88-104
July 1988

ISSN 0418-9833

Sensitivity of W' and Z' Searches at HERA [1]

F. Cornet
Max-Planck-Institut für Physik und Astrophysik,
Werner-Heisenberg-Institut für Physik
P.O.Box 40 12 12, D-8000 Munich 40, FRG

and

R. Rückl
Deutsches Elektronen-Synchrotron DESY
Notkestrasse 85, D-2000 Hamburg 52, FRG

Abstract

We study the sensitivity of deep-inelastic ep scattering at HERA to effects from hypothetical Z' and W' bosons. The explorable mass range is estimated for several interesting models. The importance of longitudinal $\epsilon^{\mp}$ beam polarization for Z' and W' searches is examined in some detail.

1 Introduction

One of the primary tasks of HERA experiments is a comprehensive study of the electroweak interactions. This includes tests of the standard model [1] as well as searches for new weak currents and bosons. The existence of additional gauge bosons associated with (spontaneously) broken symmetries is predicted by extensions of the standard theory such as left-right symmetric and grand-unified models. Also superstring theories lead, in the low-energy limit, to gauge symmetries which are generally larger than the conventional $SU(2) \times U(1)$ electroweak symmetry. The current experimental bounds on the masses of new heavy vector bosons range from

$$m_{Z'} \geq (110 - 320)\ GeV \tag{1}$$

in the case of an extra Z' [2], to

$$m_{W'} \geq (300 - 4000)\ GeV \tag{2}$$

in the case of a W' with couplings to right-handed currents [3]. Thus, from a purely experimental point of view, additional weak bosons may exist which are sufficiently light to induce observable effects in the energy range of the new accelerators.

We have investigated the prospects of detecting new weak gauge bosons at HERA. From the bounds (1) and (2), and from the low production rates for the ordinary W and Z bosons expected at HERA energies [4], it is rather clear that direct production of W' and Z' and detection in some suitable decay channels will be very difficult, if not impossible. For this reason, we concentrate on indirect searches in the neutral and charged current scattering processes, $ep \to e + X$ (NC) and $ep \to \nu + X$ (CC). Generally, one expects some changes in the standard electroweak interactions due to $Z - Z'$ and $W - W'$ mixing, and small contributions to cross-sections and other observables from the exchange of the heavier vector bosons. The absence of just such effects in existing data imposes severe constraints on the mixing angles and Z' and W' masses.

The main aim of our studies has been to improve and extend previous estimates of the explorable range of Z' and W' masses for HERA [5,6,7], and to examine more carefully how much one can gain in sensitivity if longitudinally polarized $\epsilon^{\mp}$ beams become available. We consider various E_6-type models as well as a minimal left-right symmetric model. The choice of these models is motivated by the fact that the corresponding W' and Z' bosons differ in their properties more or less strongly from the known W and Z. Thus, one also anticipates appreciable differences in the phenomenology, which makes these cases particularly interesting for our purposes. We first evaluate inclusive differential cross-sections and asymmetries for (un)polarized NC and CC $e^{\mp}p$ scattering taking $m_{Z'}$ ($m_{W'}$) and the $Z - Z'$ ($W - W'$) mixing angle as free parameters. Confronting the results with the corresponding standard model predictions we identify the most sensitive observables. The reach in $m_{Z'}$ ($m_{W'}$) through measurements of these quantities is then estimated by a χ^2 analysis of the expected deviations in comparison to experimental uncertainties.

Actually, the present analysis is only concerned with statistical errors. Systematical errors are not taken into account. However, we point out that, in the kinematical region which is important for our estimates, the systematic shifts of inclusive cross-sections can presumably be kept below 10% [8]. Furthermore, we have disregarded possible uncertainties associated with (mainly electromagnetic) radiative corrections and quark distributions. We think that the radiative effects can be properly calculated and subtracted [9]. Moreover, it is rather obvious that topics connected with strong interactions should be studied simultaneously with the electroweak physics so that a globally consistent description of the experimental results emerges. In view of the uncertainties just mentioned, asymmetries play a special role. Representing essentially ratios of cross-sections, they tend to be less affected by systematic errors, the radiative effects are smaller, and also the influence of details of the quark distributions is much weaker than in the case of cross-sections.

Numerical results will be illustrated for collisions of 30 GeV electrons and positrons with 820 GeV protons, yielding the center-of-mass energy $\sqrt{s} = 314$ GeV. Furthermore, we take an equal integrated luminosity of 250 pb^{-1} for unpolarized $e^{-}p$ and $e^{+}p$ collisions. On the other hand, for polarized $e^{\mp}_{L,R}p$ experiments we assume 80% polarization [10] and an integrated luminosity of 125 pb^{-1} per initial state.

[1] Contribution to the DESY Workshop on Physics at HERA, Hamburg, October 1987

The discussion is organized as follows. In section 2, we outline the theoretical framework and provide the formal expressions for cross-sections and asymmetries. The W' and Z' models chosen for detailed study are specified in section 3. In section 4, we describe the numerical analysis and present our results. Finally, section 5 contains some concluding remarks.

2 Theoretical Framework, Cross-Sections and Asymmetries

Models based on $SU(2)_L \times U(1) \times U(1)$ or $SU(2)_L \times SU(2) \times U(1)$ gauge symmetries represent simple, but nevertheless interesting examples for possible low energy extensions of the standard electroweak theory. Moreover, such models are particularly suitable for phenomenological studies and are therefore frequently used for just that purpose. Following our previous work [7,11] we begin with a brief discussion of NC and CC interactions in the presence of a single additional neutral boson Z' or a triplet of bosons W'_i, $i = 1,2,3$. After deriving the relevant effective lagrangians, we provide the parton model expressions for the modified differential NC and CC cross-sections as obtained in lowest order of the electroweak couplings and leading order QCD.

2.1 Neutral Current Case

The fundamental couplings of the photon, the known Z, and the new Z' to fermions are described by the effective NC lagrangian

$$\mathcal{L}_{NC} = eJ^{\mu}_{em}A_{\mu} + \frac{g}{\cos\theta_W} J^{\mu}_{Z} Z_{\mu} + g' J^{\mu}_{Z'} Z'_{\mu}, \tag{3}$$

where e and g denote the electromagnetic and the standard $SU(2)_L$ coupling constants, respectively, and g' is the new $U(1)$ (or $SU(2)$) gauge coupling. As usual, the Weinberg angle θ_W is defined by $e = g \sin\theta_W$. The currents appearing in eq. (3) have the following form:

$$J^{\mu}_{em} = \sum_f \overline{f}\gamma^{\mu} Q_f f \;\;,\;\; J^{\mu}_{Z} = \sum_f \overline{f}\gamma^{\mu}(v_f - a_f\gamma_5)f \;\;,\;\; J^{\mu}_{Z'} = \sum_f \overline{f}\gamma^{\mu}(v'_f - a'_f\gamma_5)f\;. \tag{4}$$

Here, $v_f = \frac{1}{2}T_{3f} - Q_f \sin^2\theta_W$ and $a_f = \frac{1}{2}T_{3f}$ are the vector and axial vector couplings of a fermion of flavor f to the ordinary Z, while v'_f and a'_f are the corresponding couplings of the Z'. Quite evidently, Q_f is the electric charge and T_{3f} denotes the third component of the weak isospin, e.g. for the up-quark, $Q_u = \frac{2}{3}$ and $T_{3u} = \frac{1}{2}$.

Similarly as in the standard model, spontaneous symmetry breaking can generate masses for the weak bosons. The neutral mass eigenstates will, in general, be mixtures of Z and Z' :

$$Z_1 = Z\,\cos\theta + Z'\,\sin\theta \;\;,\;\; Z_2 = -Z\,\sin\theta + Z'\,\cos\theta. \tag{5}$$

Obviously, the lighter state Z_1 is to be identified with the experimentally observed Z boson. The mixing angle θ, which depends on properties of the Higgs sector, will be treated as an essentially free parameter in order to avoid unnecessary model assumptions. However, we

do assume that the Higgs fields which acquire non-vanishing vacuum expectation values are $SU(2)_L$ doublets or singlets. In that case, the familiar relation

$$\rho = \frac{m_W^2}{m_Z^2 \cos^2\theta_W} = 1 \tag{6}$$

applies to the W and Z masses resulting in the standard model, which coincide with the physical masses of the extended models in the absence of mixing. Rewriting now eq. (3) in terms of Z_1 and Z_2 one obtains

$$\mathcal{L}_{NC} = eJ^{\mu}_{em}A_{\mu} + \frac{\epsilon}{\sin\theta_W\cos\theta_W}(J^{\mu}_1 Z_{1\mu} + J^{\mu}_2 Z_{2\mu}), \tag{7}$$

where

$$J^{\mu}_1 \;=\; \cos\theta\, J^{\mu}_Z + \sin\theta\frac{g'\cos\theta_W}{g}\, J^{\mu}_{Z'} = \sum_f \overline{f}\gamma^{\mu}(v_{1f} - a_{1f}\gamma_5)f \tag{8}$$

$$J^{\mu}_2 \;=\; -\sin\theta\, J^{\mu}_Z + \cos\theta\frac{g'\cos\theta_W}{g}\, J^{\mu}_{Z'} = \sum_f \overline{f}\gamma^{\mu}(v_{2f} - a_{2f}\gamma_5)f. \tag{9}$$

The vector and axial vector couplings v_{if} and a_{if} of the modified currents J^{μ}_i follow from

$$\begin{pmatrix} v_{1f} \\ v_{2f} \end{pmatrix} \;=\; \begin{pmatrix} \cos\theta & \sin\theta \\ -\sin\theta & \cos\theta \end{pmatrix} \begin{pmatrix} v_f \\ \frac{g'\cos\theta_W}{g} v'_f \end{pmatrix} \tag{10}$$

$$\begin{pmatrix} a_{1f} \\ a_{2f} \end{pmatrix} \;=\; \begin{pmatrix} \cos\theta & \sin\theta \\ -\sin\theta & \cos\theta \end{pmatrix} \begin{pmatrix} a_f \\ \frac{g'\cos\theta_W}{g} a'_f \end{pmatrix}. \tag{11}$$

At this point, we want to stress the effects on the standard electroweak interactions induced by $Z - Z'$ mixing. Firstly, the mass of Z_1 is lighter than the mass of the standard Z boson, as can be seen from the relation

$$\tan^2\theta = \frac{m_Z^2 - m_{Z_1}^2}{m_{Z_2}^2 - m_Z^2} \geq 0 \tag{12}$$

implied by eq. (5). Secondly, the Weinberg angle defined by the gauge couplings or, equivalently, by eq. (6) differs from the angle $\overline{\theta}_W$ obtained from the W and Z_1 mass ratio:

$$\sin^2\overline{\theta}_W \equiv 1 - \frac{m_W^2}{m_{Z_1}^2} \leq 1 - \frac{m_W^2}{m_Z^2} \equiv \sin^2\theta_W. \tag{13}$$

Thirdly, the current J^{μ}_1 which couples to the mass eigenstate Z_1 deviates from the standard neutral current J^{μ}_Z as detailed in eq. (8). Clearly, consistency with experiment requires the mixing angle θ to decrease as the mass of the heavier boson Z_2 increases.

From the lagrangian (7) one readily derives the NC cross-sections for polarized electron and positron beams. Using $Q^2 = -q^2$ and $x = -q^2/2pq$ as independent variables, where q is the four-momentum of the exchanged boson and p is the four-momentum of the incoming proton, the differential cross-sections for $e^-_{L,R}p$ scattering can be written in the form

$$\frac{d\sigma(e^-_{L,R})}{dxdQ^2} = \frac{2\pi\alpha^2}{xQ^4}\left((1 + (1-y)^2)F_2^{L,R}(x,Q^2) + (1 - (1-y)^2)xF_3^{L,R}(x,Q^2)\right) \tag{14}$$

where $y = Q^2/xs$, $\sqrt{s}$ being the total c.m. energy. The cross-sections $d\sigma(e^+_{L,R})/dxdQ^2$ for polarized positrons follow from eq. (14) after formally replacing $F_2^{L,R}$ by $F_2^{R,L}$ and $xF_3^{L,R}$ by $-xF_3^{R,L}$. Furthermore, the structure functions

$$F_2^{L,R}(x,Q^2) = \sum_f \{xq_f(x,Q^2) + x\bar{q}_f(x,Q^2)\}\tilde{F}_{2f}^{L,R}(Q^2) \quad (15)$$

$$xF_3^{L,R}(x,Q^2) = \sum_f \{xq_f(x,Q^2) - x\bar{q}_f(x,Q^2)\}\tilde{F}_{3f}^{L,R}(Q^2) \quad (16)$$

are given by scaling violating quark and antiquark density distributions q_f and $\bar{q}_f$ summed over all flavors present in the proton. The coefficients in this summation,

$$\begin{aligned}
\tilde{F}_{2f}^{L,R}(Q^2) &= Q_f^2 + \sum_{i=1}^{2}\{(v_{ie} \pm a_{ie})^2(v_{if}^2 + a_{if}^2)P_i^2 - 2Q_f(v_{ie} \pm a_{ie})v_{if}P_i\} \\
&\quad +2(v_{1e} \pm a_{1e})(v_{2e} \pm a_{2e})(v_{1f}v_{2f} + a_{1f}a_{2f})P_1P_2, \\
\tilde{F}_{3f}^{L,R}(Q^2) &= \pm 2\{\sum_{i=1}^{2}\left((v_{ie} \pm a_{ie})^2 v_{if}a_{if}P_i^2 - Q_f(v_{ie} \pm a_{ie})a_{if}P_i\right) \\
&\quad +(v_{1e} \pm a_{1e})(v_{2e} \pm a_{2e})(v_{1f}a_{2f} + a_{1f}v_{2f})P_1P_2\}, \qquad (17)
\end{aligned}$$

involve the electroweak charges and the Z_1 and Z_2 propagators. The latter are included in the factors

$$P_i = \frac{1}{\sin^2\theta_W \cos^2\theta_W}\frac{Q^2}{Q^2 + m_{Z_i}^2}. \quad (18)$$

The notation used in eq. (17) makes it easy to recognize the origin of the various contributions to the cross-sections. For unpolarized ep scattering one obviously takes the average of the left-handed and right-handed cross-sections. Strictly speaking, the above results apply to massless quarks. However, this approximation is justifiable since the bottom and top structure functions are small [12] and should have little influence on the later numerical estimates.

As promised in the introduction, we also investigate asymmetries measurable with polarized electron and positron beams. These asymmetries are defined as usual by

$$A(e_1 - e_2) = \frac{\tilde{\sigma}(e_1) - \tilde{\sigma}(e_2)}{\tilde{\sigma}(e_1) + \tilde{\sigma}(e_2)}, \quad (19)$$

where e_i denotes one of the four possible initial states, $e^{\mp}_{L,R}p$, and $\tilde{\sigma}(e_i)$ stands for the differential cross-sections $d\sigma(e_i)/dxdQ^2$ described above. In the case of asymmetries integrated over x, we substitude $d\sigma(e_i)/dQ^2$ for $\tilde{\sigma}(e_i)$. As a matter of fact, ep collisions give access to six asymmetries of different kind: polarization asymmetries $A(e^-_L - e^-_R)$ and $A(e^+_L - e^+_R)$, charge asymmetries $A(e^-_L - e^+_L)$ and $A(e^-_R - e^+_R)$, and mixed asymmetries $A(e^-_L - e^+_R)$ and $A(e^-_R - e^+_L)$. Sometimes, we will also use the shorthand $A^{--}_{L,R}$, A^{++}_{LR}, etc.. Obviously, since there are only four independent cross-sections, only four of these asymmetries are independent. Nevertheless, it is very useful to consider all of them in order to get the best possible bounds for different Z' species, and to distinguish the various models in case a signal is detected.

2.2 Charged Current Case

The CC interactions in the presence of $W'^{\pm}$ bosons associated with an additional $SU(2)$ gauge symmetry can be treated very similarly to the NC case just described. Starting from the CC lagrangian in the form

$$\mathcal{L}_{CC} = \frac{g}{2\sqrt{2}}J^{\mu}_W W_{\mu} + \frac{g'}{2\sqrt{2}}J^{\mu}_{W'}W'_{\mu} + c.c. \ , \quad (20)$$

where g and g' are the coupling constants of the standard $SU(2)_L$ and the new $SU(2)$ gauge group, respectively, and defining the charged mass eigenstates W_1 and W_2 by

$$W_1 = W\cos\zeta + W'\sin\zeta \ , \quad W_2 = -W\sin\zeta + W'\cos\zeta, \quad (21)$$

one arrives at the effective lagrangian

$$\mathcal{L}_{CC} = \frac{g}{2\sqrt{2}}(J^{\mu}_1 W_{1\mu} + J^{\mu}_2 W_{2\mu}) + c.c. \ , \quad (22)$$

where

$$J^{\mu}_1 = \cos\zeta\ J^{\mu}_W + \sin\zeta\frac{g'}{g}\ J^{\mu}_{W'} \quad (23)$$

$$J^{\mu}_2 = -\sin\zeta\ J^{\mu}_W + \cos\zeta\frac{g'}{g}\ J^{\mu}_{W'}. \quad (24)$$

In the above, J^{μ}_W is the standard left-handed charged current,

$$J^{\mu}_W = \sum_{i,j}[\bar{\nu}_i\gamma^{\mu}(1-\gamma_5)\delta_{ij}e_j + \bar{u}_i\gamma^{\mu}(1-\gamma_5)V_{ij}d_j], \quad (25)$$

i and j being family indices (e.g. $e_1 = e$, $e_2 = \mu$, $u_1 = u$, $u_2 = c$, etc.) and V_{ij} denoting the Kobayashi-Maskawa mixing matrix. In contrast, the new current $J^{\mu}_{W'}$ can have a more general structure, analogous to $J^{\mu}_{Z'}$ in eq. (4). However, for simplicity we shall proceed directly to the particularly interesting case of a left-right symmetric scenario [13]. Then, introducing right-handed neutrino fields and adopting the usual multiplet assignment under $SU(2)_R$ for the fermions, one has

$$J^{\mu}_{W'} = \sum_{i,j}[\bar{\nu}_i\gamma^{\mu}(1+\gamma_5)\delta_{ij}e_j + \bar{u}_i\gamma^{\mu}(1+\gamma_5)V'_{ij}d_j], \quad (26)$$

where we have made the reasonable assumption that mixing among lepton species is negligible, and introduced the matrix V'_{ij} to describe mixing in the right-handed quark sector.

Using eqs. (22-26) it is straightforward to calculate the inclusive CC cross-sections for polarized $e^{\mp}_{L,R}p$ scattering. In the limit of massless quarks and for a sufficiently light right-handed electron neutrino [14], one obtains

$$\frac{d\sigma(e^-_{L,R})}{dxdQ^2} = \frac{\pi\alpha^2}{2\sin^4\theta_W}\sum_i\{u_i(x,Q^2)[A^{L,R} + (1-y)^2B] + \bar{d}_i(x,Q^2)[B + (1-y)^2A^{L,R}]\}, \quad (27)$$

and

$$\frac{d\sigma(e^+_{L,R})}{dxdQ^2} = \frac{\pi\alpha^2}{2\sin^4\theta_W}\sum_i\{\overline{u}_i(x,Q^2)[A^{R,L}+(1-y)^2B]+d_i(x,Q^2)[B+(1-y)^2A^{R,L}]\}, \quad (28)$$

with

$$\begin{aligned} A^L(Q^2) &= (\cos^2\zeta P_1+\sin^2\zeta P_2)^2 \\ A^R(Q^2) &= (\sin^2\zeta P_1+\cos^2\zeta P_2)^2(\frac{g'}{g})^4 \\ B(Q^2) &= \sin^2\zeta\cos^2\zeta(P_1-P_2)^2(\frac{g'}{g})^2. \end{aligned} \quad (29)$$

Here, the quantities $P_i = 1/(Q^2+m^2_{W_i})$, $i=1,2$, refer to the W_1 and W_2 propagators. Moreover, because of unitarity, the quark mixing matrices V_{ij} and V'_{ij} drop out from the sum over all quark flavors in the final state. In practice, we shall only include u,d,s, and c quark flavors in our estimates, similarly as for the NC cross-sections. Nevertheless, one may use the above formulas provided that the right-handed mixing matrix is almost unitary in the (u,d,s,c)-sector as it is known to be the case for the usual KM matrix.

The main results of this section are summarized in eqs. (17) and (29). One can see from these expressions the twofold effect that additional Z' and W' bosons have on ep collisions: deviations of the interactions involving the lighter bosons from the standard model due to $Z-Z'$ and $W-W'$ mixing, and additional contributions from the exchange of the heavier bosons. Both of these effects decrease as the masses of the heavier states increase such that the standard model is recovered in the limit $m_{Z_2,W_2}\to\infty$.

3 Specification of Z' and W' Models

Having outlined the general formalism, we shall now specify the models chosen for numerical study. The idea is to select models which are well motivated theoretically and which, from an experimental point of view, represent relatively easy as well as more difficult possibilities. One can then hope to get an adequate overall-picture of the prospects of Z' and W' searches at HERA.

3.1 E_6 Models with One Z' at Low Energies

One class of models we want to study is suggested by superstring phenomenology [15] and thus has recently received great attention. Roughly speaking, compactification of the heterotic $E_8\times E'_8$ superstring in 10 dimensions may lead to a supersymmetric E_6 theory in 4 dimensions with the E_6 symmetry broken to some subgroup G at the Planck scale. If there is no further symmetry breaking at intermediate scales, that is if G is the low energy group, it must necessarily be bigger than the gauge group of the standard model. This leaves $SU(3)_C\times SU(2)_L\times U(1)_Y\times U(1)_{Y'} = G\subset E_6$ as the minimal low energy theory containing the standard model. In case G is some bigger subgroup of E_6, the above minimally extended electroweak model could result from intermediate stages of symmetry breaking. Furthermore,

it is assumed that the extra $U(1)_{Y'}$ breaks down at a relatively low scale of $O(1\ TeV)$ in which case the Z' may acquire a mass $m_{Z'}\le O(1\ TeV)$. For the effective $U(1)_{Y'}$ gauge coupling we take the value

$$g_{Y'} = \sqrt{\frac{5}{3}}\frac{e}{\cos\theta_W} \quad (30)$$

which is normalized such that in the E_6 symmetry limit, when $\sin^2\theta_W = 3/8$, $g_{Y'}$ is equal to the $SU(2)_L$ coupling $g = e/\sin\theta_W$.

In general, there is an infinite number of possible $U(1)$ subgroups of E_6 which may play the role of the additional low energy gauge group $U(1)_{Y'}$. The point is that E_6 has rank 6 and thus contains two $U(1)$'s in addition to $SU(3)_C\times SU(2)_L\times U(1)_Y$ which has rank 4. Decomposing E_6 as indicated below,

$$\begin{aligned} E_6 &\subset SO(10)\times U(1)_\psi \subset SU(5)\times U(1)_\chi\times U(1)_\psi \\ &\subset SU(3)_C\times SU(2)_L\times U(1)_Y\times U(1)_\chi\times U(1)_\psi, \end{aligned} \quad (31)$$

one can represent the $U(1)_{Y'}$ as a linear combination of $U(1)_\chi$ and $U(1)_\psi$ [16]. Correspondingly, one may consider the Z' boson associated with $U(1)_{Y'}$ as a superposition of the $U(1)_\psi$ and $U(1)_\chi$ gauge fields Z^μ_ψ and Z^μ_χ, respectively:

$$Z'^\mu = Z^\mu_\psi\cos\alpha + Z^\mu_\chi\sin\alpha. \quad (32)$$

The angle α can then conveniently be used to specify a particular model of this class.

The assignment of the $U(1)_{Y'}$ charges to the fermions is fixed as explained below. The 15 helicity components of a standard lepton and quark family form, together with new fermion species, a fundamental 27-plet of E_6 which contains the following $(SO(10),SU(5))$-representations:

$$\underline{27} = (\underline{16},\underline{10}+\underline{5}^*+\underline{1})+(\underline{10},\underline{5}+\underline{5}^*)+(\underline{1},\underline{1}). \quad (33)$$

The known fermions $\{u_L,d_L,u^c_L,e^c_L\}$ and $\{d^c_L,\nu_L,e_L\}$ fill the $(\underline{16},\underline{10})$ and $(\underline{16},\underline{5}^*)$ multiplets, respectively. The heavier families possess an analogous multiplet structure. Parametrizing the $U(1)_{Y'}$ charges of the fermions in accordance with eq.(32), one has

$$Y'_f = Y^\psi_f\cos\alpha + Y^\chi_f\sin\alpha, \quad (34)$$

where $Y^\psi_f[Y^\chi_f]$ denote the $U(1)_\psi[U(1)_\chi]$ charges given below for the multiplets appearing in eq.(33):

E_6	$\underline{27}$					
$SO(10)$	$\underline{16}$			$\underline{10}$		$\underline{1}$
$\sqrt{6}Y^\psi$	$1/2$			-1		2
$SU(5)$	$\underline{10}$	$\underline{5}^*$	$\underline{1}$	$\underline{5}$	$\underline{5}^*$	$\underline{1}$
$\sqrt{10}Y^\chi$	$1/2$	$-3/2$	$5/2$	-1	1	0

We have selected the following three possibilities [17]:

$$\begin{array}{lll} \text{model A:} & \cos\alpha = \sqrt{\frac{5}{8}} & , \ \sin\alpha = \sqrt{\frac{3}{8}} \ , \\ \text{model B:} & \cos\alpha = 0 & , \ \sin\alpha = 1 \ , \\ \text{model C:} & \cos\alpha = -\sqrt{\frac{15}{16}} & , \ \sin\alpha = \sqrt{\frac{1}{16}} \ . \end{array} \tag{35}$$

Model A is unique in the sense that it corresponds to the minimal scenario $E_6 \supset G = SU(3)_C \times SU(2)_L \times U(1)_Y \times U(1)_{Y'}$ favored by no-scale supergravity models [18], while models B and C involve symmetry breaking at intermediate scales triggered by a $(\underline{1},\underline{1})$ and a $(\underline{16},\underline{1})$ scalar field, respectively. The hypercharges Y' for models A to C follow from eq. (34) and the above table. Since the exotic fermions in the fundamental $\underline{27}$-representation of E_6 are irrelevant for ep scattering at HERA energies, we only state the charges of the ordinary leptons and quarks:

$$\begin{array}{lll} Y'(u_L, d_L, u_L^c, e_L^c) & = & 1/\sqrt{15} \ \ (\text{A}), \ \ 1/2\sqrt{10} \ \ (\text{B}), \ \ -1/2\sqrt{10} \ \ (\text{C}), \\ Y'(d_L^c, \nu_L, e_L) & = & 1/2\sqrt{15} \ \ (\text{A}), \ \ -3/2\sqrt{10} \ \ (\text{B}), \ \ -1/\sqrt{10} \ \ (\text{C}). \end{array} \tag{36}$$

The charges of the heavier fermion families are assigned correspondingly. Furthermore, the Z' vector (v'_f) and axialvector (a'_f) couplings in eqs.(10) and (11) are to be substituded by

$$v'_f = \frac{1}{2}(Y'_{f_L} - Y'_{f_L^c}), \ \ a'_f = \frac{1}{2}(Y'_{f_L} + Y'_{f_L^c}). \tag{37}$$

Finally, it is interesting to note that the Higgs fields also belong to a $\underline{27}$-plet of E_6 which contains only $SU(2)_L$ doublets and singlets. Hence, the relation (6) is naturally fullfilled in this class of models.

3.2 Left-Right Symmetric Model

Left-right symmetric models [13] are motivated by the attempt to understand P and C violations in weak interactions. The general idea is to start with an electroweak lagrangian which, before spontaneous symmetry breaking, is P and C conserving, and to attribute the observed P and C violations to the non-invariance of the vacuum. The simplest realization of this idea is based on the gauge group

$$SU(2)_L \times SU(2)_R \times U(1)_{B-L}. \tag{38}$$

Moreover, it is natural to assume a discrete symmetry under the interchange of L and R, so that

$$g = g' = \frac{\epsilon}{\sin\theta_W} \tag{39}$$

where g and g' are the $SU(2)_L$ and $SU(2)_R$ gauge couplings, respectively. In this model one has a second isotriplet vector field, $W'_{1,2,3}$, associated with $SU(2)_R$, in addition to the the standard $SU(2)_L$ gauge field $W_{1,2,3}$ and the singlet field related to $U(1)_{B-L}$. After symmetry breaking all vector bosons, except the photon, acquire a mass. The mass eigenstates can be described as mixtures of Z and Z', and $W^{\pm}$ and $W'^{\pm}$, according to eqs. (5) and (21).

The fermions transform under the group (38) as follows. The left-handed components are doublets under $SU(2)_L$ and singlets under $SU(2)_R$, while the right-handed components (which now include also right-handed neutrinos) form singlets under $SU(2)_L$ and doublets under $SU(2)_R$. The electric charge is given by

$$Q = T_{3_L} + T_{3_R} + \frac{B-L}{2} \ . \tag{40}$$

where $T_{3_{L,R}}$ denote the weak isospin quantum numbers, and B and L are the baryon and lepton numbers, respectively. The $U(1)$ generator, being proportional to $B-L$, has thus a simple physical interpretation in this model. The complete assignment of leptons and quarks is summarized below:

$$\begin{array}{lll} l_L & = & (\frac{1}{2}, 0, -1), \ \ l_R \ = \ (0, \frac{1}{2}, -1), \\ q_L & = & (\frac{1}{2}, 0, \frac{1}{3}), \ \ \ q_R \ = \ (0, \frac{1}{2}, \frac{1}{3}). \end{array} \tag{41}$$

It is now straightforward to derive the vector and axialvector couplings v'_f and a'_f for the second neutral boson which, together with the gauge coupling g' from eq. (39), have to be used in $\mathcal{L}_{NC}$ as given by eqs. (3) and (4). For the particular model specified above, one finds [19]

$$\begin{array}{lll} v'_f & = & \frac{1}{\cos\theta_W \sqrt{\cos 2\theta_W}} (\frac{1}{2} T_{3f} - \sin^2\theta_W Q_f) \\ a'_f & = & -\frac{\sqrt{\cos 2\theta_W}}{\cos\theta_W} (\frac{1}{2} T_{3f}). \end{array} \tag{42}$$

As far as the CC interactions are concerned, one can directly use the results of section 2.2 after putting $\frac{g'}{g} = 1$ in eqs. (23), (24) and (29), in accordance with the assumption (39).

4 Numerical Studies and Results

We have already said that in NC and CC processes, $ep \to lX$, the existence of new weak bosons manifests itself mainly in deviations of inclusive measurements from the predictions of the standard theory. The deviations are expected to be largest at high values of Q^2, and to disappear gradually as Q^2 decreases. As it turns out, they do not depend very much on Bjorken-x. Therefore, we have concentrated on tests through measurements of Q^2-distributions in the range $Q^2 \geq 1000$ GeV^2. In a comprehensive study of the inherent sensitivity of differential cross-sections and asymmetries, we have first identified the most favorable observables for each of the models specified in the last section. Some illustrative examples will be shown in the following. Using the outcome of this survey, we estimate sensitivity limits by a χ^2 analysis of the expected deviations from the standard model in comparison to statistical measurement errors.

More precisely, for a given observable F we calculate

$$\chi^2(m_2) = \sum_{\text{bins in } Q^2} \left(\frac{F(m_2) - F_{SM}}{\delta F} \right)^2 , \tag{43}$$

where $F(m_2)$ denotes the prediction of a particular two-Z or two-W model as a function of the mass of the heavier vector boson, F_{SM} is the result expected in the standard model, and δF is the estimated statistical uncertainty. By definition, $\chi^2(m_2) \to 0$ as $m_2 \to \infty$. Thus, using the χ^2 distribution with one degree of freedom one can consider the hypothesis of the presence of a second boson with mass m_2 excluded at the 90 % confidence level if $\chi^2(m_2) < 2.7$. Although this procedure is rather rough, it should permit a reasonable evaluation of the experimental reach at HERA.

The numerical results which will be presented in this section are obtained with the formulas summarized in section 2. Furthermore, for the quark density distributions we have used the Duke and Owens parametrization I [20], and for the electroweak parameters in the standard model we have taken the values

$$\alpha = \frac{1}{137},\ m_Z = 93.3\ GeV,\ m_W = 82.4\ GeV,\ \sin^2\theta_W = 0.22. \qquad (44)$$

The treatment of the electroweak parameters in the extended models is explained below.

4.1 Effects from Z' and Sensitivity Limits

The Z' models as specified so far still involve four parameters: the vector boson masses m_{Z_1} and m_{Z_2}, the Z-Z' mixing angle θ, and the Weinberg angle θ_W. The lower mass m_{Z_1} is assumed to be known experimentally with great precision (e.g. from measurements at LEP) and is therefore kept fixed at $m_{Z_1} = 93.3\ GeV$, the value also adopted for the standard model. Furthermore, putting $m_W = 38.65\ GeV/\sin\theta_W$ and m_Z from eq.(12) in the constraint (6), one obtains the Weinberg angle as a function of m_{Z_2} and θ. The above relation for m_W includes the usual radiative corrections [21], but neglects the contributions from new particles in the models, an approximation which suffices for the present purposes. Finally, m_{Z_2} and θ, being related to uncertain vacuum expectation values of Higgs fields [6,17], are treated as free parameters. Of course, the existing measurements of $\sin^2\theta_W$ imply some contraints [2] as shown later. Following this strategy we have investigate the deviations of the E_6 models A, B, and C and the left-right symmetric model (LR) from the standard model in the (m_{Z_2}, θ)-plane.

Quite generally, one can say that tests with polarized $e^\mp$ beams are more powerful than unpolarized measurements. In particular, the NC asymmetries defined in eq.(19) are rather sensitive quantities and have the further advantages that systematic errors on the cross-sections partly cancel, that the influence of uncertainties connected with the quark structure functions is greatly reduced, and that the electroweak radiative corrections are relatively small [9]. To examine the sensitivity of polarization, charge and mixed asymmetries we compute the contours in the (m_{Z_2}, θ)-plane for which the standard model predictions $A_{SM}(\epsilon_1 - \epsilon_2)$ differ from the asymmetries $A(\epsilon_1 - \epsilon_2)$ expected in the two-Z models by $\delta A = |A(\epsilon_1 - \epsilon_2) - A_{SM}(\epsilon_1 - \epsilon_2)| = 0.04$. The results are shown in Fig. 1 for the most sensitive asymmetry of each kind. For this illustration we have chosen suitable values for x and Q^2 which are experimentally accessible with reasonable statistics. Measurements with a precision $\delta A = 0.04$ would allow to explore the regions in m_{Z_2} and θ outside the contours. The following observations are noteworthy:

(1) The sensitivity depends strongly on the Z' model as well as on the asymmetry considered.

(2) The 'vertical' contours mainly reflect the deviations of Z_1 from the standard model Z due to $Z - Z'$ mixing, while the 'horizontal' contours are also sensitive to Z_2.

(3) The mixing effects are not very model-specific, whereas the deviations in asymmetries due to Z_2 exchange clearly discriminate between models. However, the latter effects are only substantial for a relatively light Z_2.

The above results underline the importance of studying different asymmetries in order to optimize the chances for discovery, to distinguish the existence of a new Z' from other possible sources of an effect which might be seen, and to determine properties of the Z'.

Also shown in Fig. 1 are boundaries in (m_{Z_2}, θ) derived from a global analysis of available data on NC processes [2]. One can see that for models A and LR the lower bounds on m_{Z_2} can be considerably improved at HERA, provided a shift $\delta A = 0.04$ in asymmetries can be detected. On the other hand, in the case of model B one seems to gain very little from asymmetry measurements, while model C is rather difficult to test at all. Another lesson which can be learned from Fig. 1 is that existing data already exclude sizeable $Z - Z'$ mixing, at least in the upper range of masses interesting at HERA. In the subsequent studies we will therefore neglect mixing and take $\theta = 0$.

A drawback of asymmetry tests is the necessity to share luminosity among runs with $\epsilon^\mp_{L,R}$ beams. Fig. 2 illustrates the statistical significance for an integrated luminosity of 125 pb^{-1} per polarization state and 100% beam polarization. We have plotted the standard model predictions for selected asymmetries, integrated over x, together with the corresponding asymmetries expected in the E_6 models for $m_{Z_2} = 200$ GeV and in the LR model for $m_{Z_2} = 500$ GeV. The differences should be compared with the statistical errors which are also indicated. In order to ensure a sufficient number of events in each Q^2-bin, we have increased the bin size with Q^2 taking equal bins on a logarithmic scale, namely $\Delta \log Q^2 = 0.2$. One can infer from Fig. 2 that, from the point of view of statistics, it should be possible to probe models A and B up to masses around 200 GeV, and model LR up to masses around 500 GeV. On the other hand, model C produces barely observable effects, even for masses below 200 GeV as expected from Fig. 1. It is interesting, but maybe not surprising, to note that E_6 models are more difficult to test experimentally than left-right symmetric models or a simple heavier repetition of the standard Z. Reasons for that are the relatively weak Z' couplings (eq. (30) in comparison to eq. (39)) and cancellations among the $\gamma - Z$ and $\gamma - Z'$ interference contributions which generally give rise to the dominant effects.

Let us now turn to the main results of our analysis: the quantitative estimates of sensitivity limits for m_{Z_2} on the basis of the χ^2 function defined in eq. (43). We have calculated χ^2 versus m_{Z_2} for the unpolarized cross-sections $d\sigma(e^-p)/dQ^2$ and $d\sigma(e^+p)/dQ^2$ and for the various asymmetries in polarized $e^\mp_{L,R}$ scattering assuming, more realistically, 80% polarization. The sum in eq. (43) is taken over the Q^2-bins considered in Fig. 2. Fig. 3 shows the results for the cross-sections and asymmetries which give the largest χ^2. We find that NC asymmetries provide more sensitive tests than unpolarized cross-sections. This is true for all models considered, with the exception of model B which is best probed in unpolarized e^+p scattering. In the following table, we summarize the bounds on m_{Z_2} (in GeV) at 90% c.l. which can

be expected from HERA under the assumptions leading to Fig. 3. Also indicated are the observables from which these estimates are derived, and the 90% c.l. lower limits on m_{Z_2} as obtained from a combined analysis of existing NC data [2].

model	unpol. measurement		'best' measurement		present lower limits
A	180	$(\frac{d\sigma(e^-)}{dQ^2})$	200	(A_{LR}^{--})	110
B	300	$(\frac{d\sigma(e^+)}{dQ^2})$	300	$(\frac{d\sigma(e^+)}{dQ^2})$	270
C		-	130	(A_{LL}^{-+})	-
LR	350	$(\frac{d\sigma(e^-)}{dQ^2})$	470	(A_{RR}^{-+})	320

4.2 Sensitivity Limits for a W' Coupled to Right-Handed Currents

A W' boson which couples to right-handed currents gives rise to the process $ep \to \nu_R X$. The nature (Dirac or Majorana fermion) and mass ($m_{\nu_R} \ll$ or $\approx m_{W'}$) of the right-handed neutrino, if it exists, is not known. If ν_R is a sufficiently heavy Majorana particle, it decays with equal probability into $e^- + X$ and $e^+ + X$ and thus provides a spectacular signature at an ep collider [14]. However, in view of the existing bounds on $m_{W'}$, this possibility is not very likely to occur at HERA, at least not for the theoretically favored case, $m_{\nu_R} \approx m_{W'}$. On the other hand, if ν_R is a light Dirac particle, there is no final state signature so that one has to rely on indirect searches as in the case of a Z'.

Considering the latter possibility and using the model defined in section 3.2, we have investigated tests using polarized and unpolarized cross-sections as well as the ratios $R^- = \tilde{\sigma}(e_R^-)/\tilde{\sigma}(e_L^-)$ and $R^+ = \tilde{\sigma}(e_L^+)/\tilde{\sigma}(e_R^+)$ [22] where $\tilde{\sigma} \equiv d\sigma/dQ^2$. If one makes the same assumptions on luminosity and degree of polarization as in the Z' study and applies eq. (43), one finds the χ^2 functions shown in Fig. 4. On purely statistical grounds, the most sensitive tests are provided by $d\sigma(e_R^-)/dQ^2$ and R^-. Below, we summarize our estimates on the bounds (in GeV) which could be put on $m_{W'}$ if no effect is observed at the 90% c.l., together with the least model-dependent present limit [3].

from $d\sigma(e^-)/dQ^2$	from $d\sigma(e_R^-)/dQ^2$ or R^-	present lowest limit
300	400	300

5 Summary

We have studied the sensitivity of searches for new Z' and W' gauge bosons in the inclusive processes, $ep \to eX$ and $ep \to \nu X$, at the HERA energy of 314 GeV in the center-of-mass. Besides obvious tests with unpolarized $e^\mp$ beams, we have also investigated possibilities which exist if longitudinally polarized $e^\mp_{L,R}$ beams are available. The main manifestations of additional weak bosons consist in small deviations of cross-sections and asymmetries from the values predicted by the standard model, in particular, in the high Q^2 region. Since the event rates drop off rapidly with Q^2, high luminosity is essential for successful searches. We have assumed an integrated luminosity of 250 pb^{-1} for unpolarized cross-section measurements and

half as much for measurements of polarized cross-sections. Another important prerequisite is a high degree of polarization. We have assumed 80%, a number which is close to the theoretically possible maximum [10].

With the above assumptions we have estimated sensitivity limits in terms of 90% c.l. bounds on the masses of Z' and W' which could be obtained from various tests if no effect is observed. It should be stressed, however, that only statistical errors are taken into account. Our main results can be summarized as follows:

(i) The sensitivity to new weak bosons depends rather strongly on their properties, i.e. on the particular model considered.

(ii) Tests with polarized lepton beams are generally more powerful than searches without polarization. However, we have also noticed exceptions from this rule.

(iii) For the particular E_6 and L-R models used as illustrative examples, we find that without polarization one can reach masses up to about 350 GeV. This range can be extended by 10 to 40 % with the help of polarized beams.

(iv) Maybe more importantly, in case a signal is observed, polarization experiments are most efficient in determining Z' and W' couplings and distinguishing models.

(v) $Z - Z'$ and $W - W'$ mixing is already strongly constrained by existing data so that we do not expect to gain further limits on mixing angles from HERA.

A final remark concerns systematical errors. Their influence remains of course to be seen. At present, it is very difficult to include the systematics realistically. However, it should be possible to keep the impact on Z' and W' searches at an acceptable level by normalizing theory to experiment in the lower Q^2 region, where no deviations from the standard model are expected, and using only high Q^2 data to test a given hypothesis. The sensitivity may then essentially be limited by statistics so that our estimates apply.

Acknowledgements. We thank J. Blümlein, G. Ingelman, H. Kowalski, R.D. Peccei and G. Wolf for helpful discussions.

References

[1] J. Blümlein, G. Cozzika, O. Gry, D. Haidt, G.D. Heath, G. Ingelman, M. Klein, E. Paul, T. Riemann, these Proceedings

[2] U. Amaldi et al., Phys. Rev. D36 (1987) 1385

[3] P. Langacker, Proc. of the 1985 Int. Symp. on Lepton and Photon Interactions at High Energies, eds. M. Konuma, K. Takahashi (Kyoto University, Kyoto, 1986) p. 186

[4] K.J.F. Gaemers, R.M. Godbole, M. van der Horst, these Proceedings

[5] E. Longo, Proc. of the Workshop Experimentation at HERA, NIKHEF Amsterdam, 1983, DESY HERA 83/20, p. 285
R.J. Cashmore et al., Phys. Rep. 122 (1985) 275
R. Rückl, Proc. of the ECFA Workshop on LEP 200, Aachen, 1986, eds. A. Böhm, W. Hoogland, CERN 87-08, p. 453

[6] V.D. Angelopoulos, J. Ellis, D.V. Nanopoulos, N.D. Tracas, Phys. Lett. 176B (1986) 203

[7] F. Cornet, R. Rückl, Phys. Lett. 184B (1987) 263

[8] J. Feltesse, these Proceedings

[9] H. Spiessberger, these Proceedings
J. Kripfganz, H.J. Möhring, Z. Phys. C38 (1988) 653

[10] D.P. Barber, Proc. of the 7. Int. Symp. on High Energy Spin Physics, Protvino, USSR, 1986 (Institute for High Energy Physics, Serpukhov, 1987) (DESY 86-170), and
Proc. of the Adriatic Research Conf. on Spin and Polarization Dynamics in Nuclear and Particle Physics, ICTP Trieste, 1987 (to appear in Physica Scripta)

[11] F. Cornet, R. Rückl, Proc. of the Workshop on Physics at Future Accelerators, La Thuile and Geneva, 1987, ed. J.H. Mulvey, CERN 87-07, Vol.II, p.190

[12] M. Glück, R.M. Godbole, E. Reya, Z. Phys. C38 (1988) 441
M. Glück, these Proceedings

[13] For a review see, e.g.
R.N. Mohapatra, Quarks and Leptons and Beyond, eds. H. Fritzsch, R.D. Peccei, H. Saller, F. Wagner (Plenum Press, New York, 1985) p. 219

[14] The case of heavy right-handed neutrinos is discussed, for example, in
G. Altarelli, B. Mele, R. Rückl, Proc. of the ECFA-CERN Workshop on a Large Hadron Collider in the LEP Tunnel, Lausanne and Geneva, 1984, ed. M. Jacob, CERN 84-10, Vol.II, p.549

[15] for reviews see, e.g.
R.D. Peccei, Proc. of the 23rd Int. Conf. on High Energy Physics, Berkeley, 1986, ed. S.C. Loken (World Scientific Pub. Co., Singapore, 1987) p. 3.

G.G. Ross, Proc. of the 1987 Int. Symp. on Lepton and Photon Interactions at High Energies, Hamburg, eds. W. Bartel, R. Rückl, (North- Holland Physics Pub., Amsterdam, 1988) p. 743

[16] D. London, J.L. Rosner, Phys. Rev. D34 (1986) 1530.

[17] F. del Aguila, M. Quiros, F. Zwirner, Proc. of the Workshop on Physics at Future Accelerators, La Thuile and Geneva, 1987, ed. J.H. Mulvey, CERN 87-07, Vol.II, p.165, and Nucl. Phys. B287 (1987) 419

[18] E. Cohen, J. Ellis, K. Enquist, D.V. Nanopoulos, Phys. Lett. 165B (1985) 76

[19] V. Barger, E. Ma, K. Whisnant, Phys. Rev. D26 (1982) 2378 and D28 (1983) 1618
M.J. Duncan, P. Langacker, Nucl. Phys. B277 (1986) 285

[20] D.W. Duke, J.F. Owens, Phys. Rev. D30 (1984) 49

[21] W.J. Marciano, A. Sirlin, Phys. Rev. D22 (1980) 2695

[22] E. Longo, Proc. of the Workshop Experimentation at HERA, NIKHEF Amsterdam, 1983, DESY HERA 83/20, p. 285

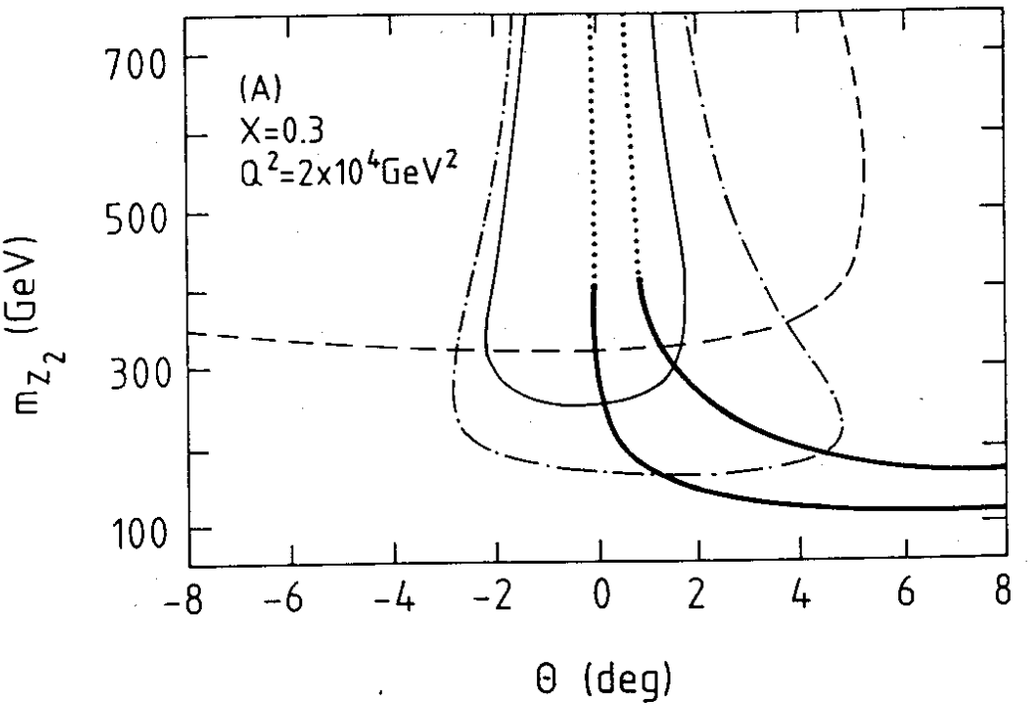

Figure 1a
Contours showing the values of m_{Z_2} and θ for which the asymmetries A_{LR}^{--} (full), A_{RR}^{-+} (dash-dotted), and A_{RL}^{-+} (dashed) obtained in model A deviate from the standard model predictions by $\delta A = 0.04$. Existing NC data constrain m_{Z_2} and θ for this model to the region inside the boundaries indicated by thick lines [2]

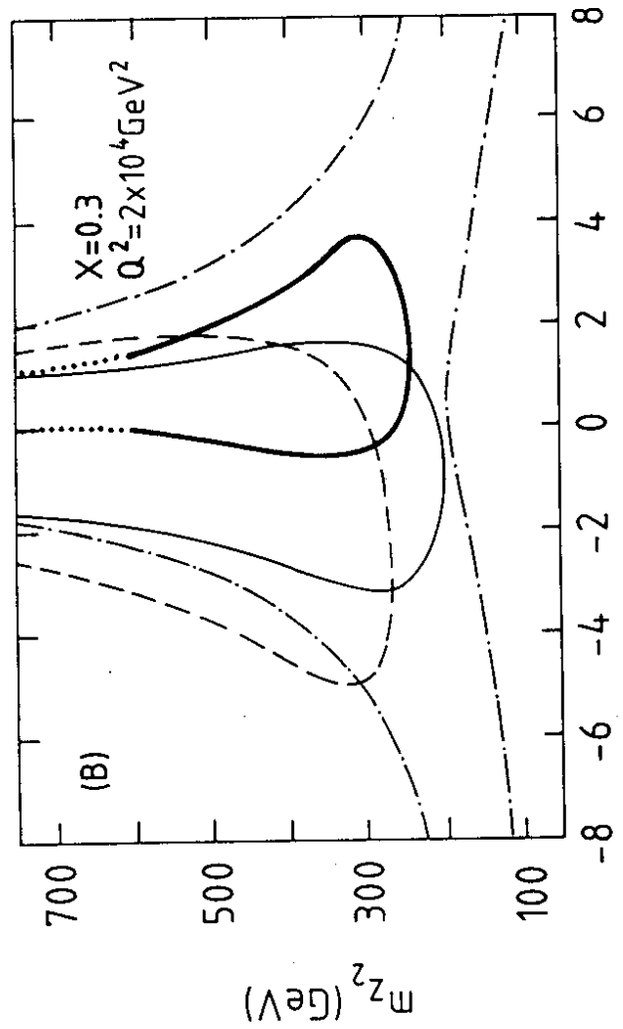

Figure 1b
Same as Fig. 1a, for model B and the asymmetries A_{LR}^{--} (full), A_{RR}^{-+} (dash-dotted), and A_{LR}^{-+} (dashed)

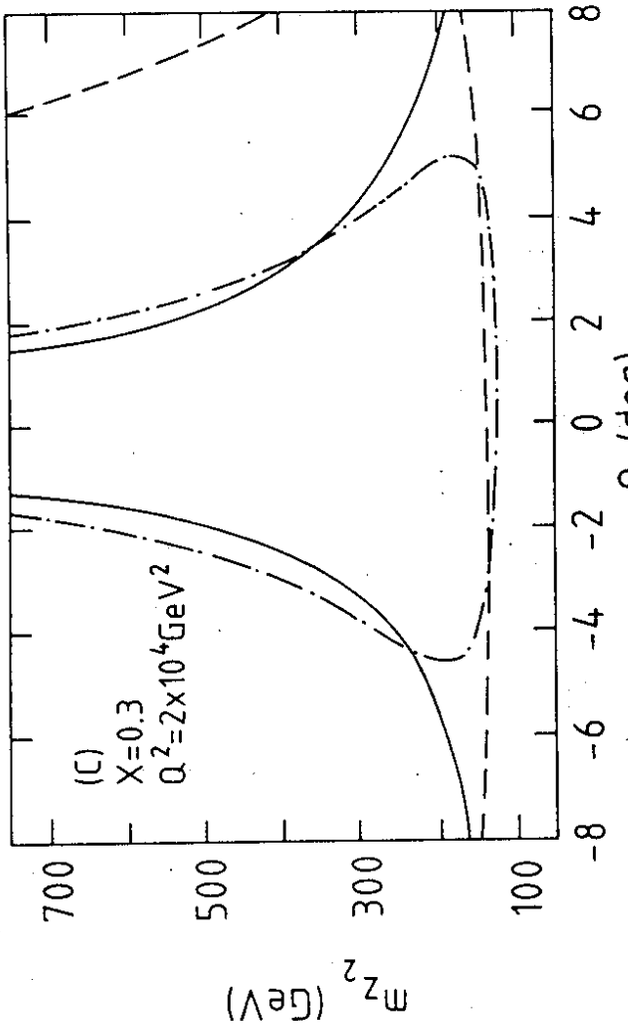

Figure 1c
Same as Fig. 1a, for model C (we are not aware of published bounds in this case)

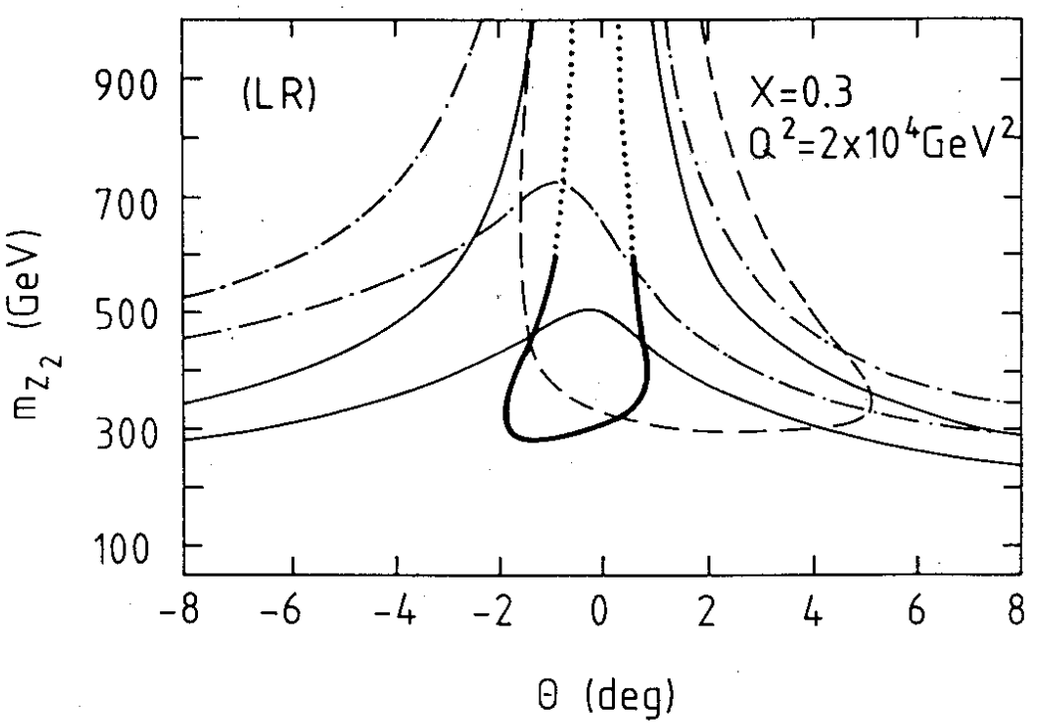

Figure 1d
Same as Fig. 1a, for the left-right symmetric model and the asymmetries A_{LR}^{--} (full), A_{RR}^{++} (dash-dotted), and A_{LR}^{-+} (dashed)

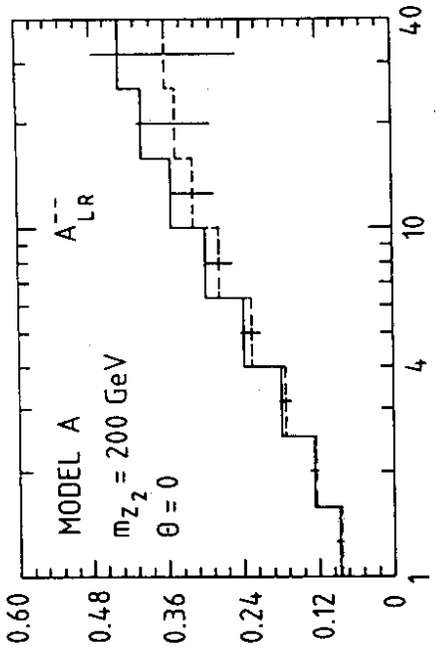

Figure 2a
Polarization asymmetry A_{LR}^{--}, integrated over π, for model A (full) in comparison to the standard model prediction (dashed). The error bars indicate the statistical uncertainties for an integrated luminosity of 125 pb^{-1} per polarized beam. The degree of polarization is assumed to be 100%

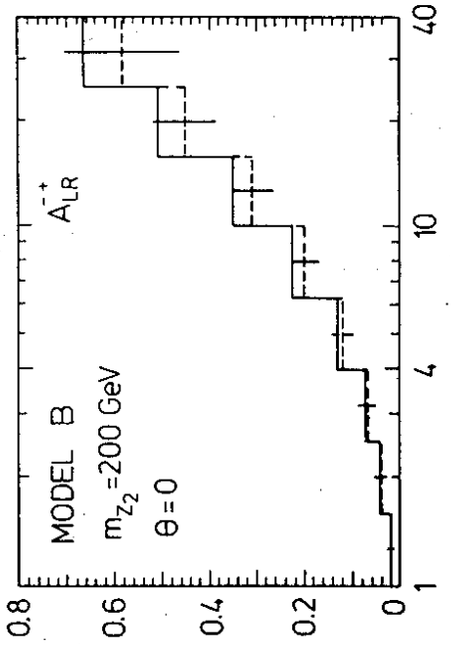

Figure 2b
Same as Fig. 2a, for the mixed asymmetry A_{LR}^{-+} and model B

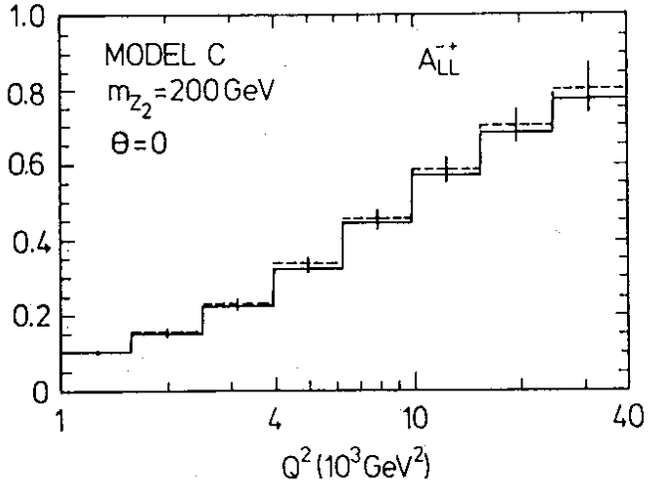

Figure 2c
Same as Fig. 2a, for the charge asymmetry A_{LL}^{-+} and model C

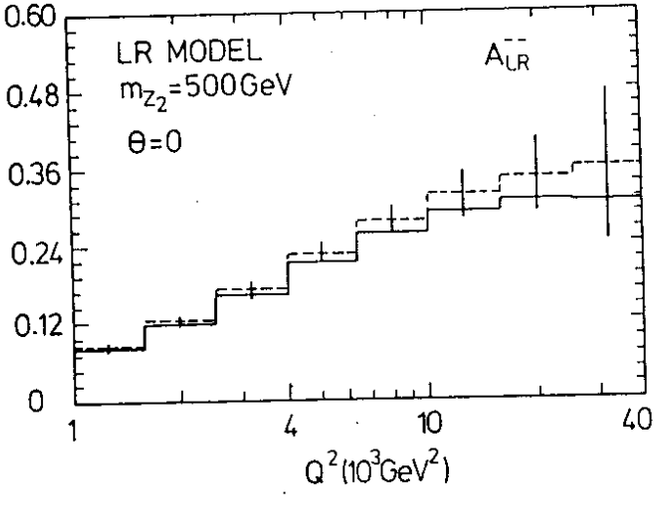

Figure 2d
Same as Fig. 2a, for the left-right symmetric model
(note the higher value of m_{Z_2} in this case)

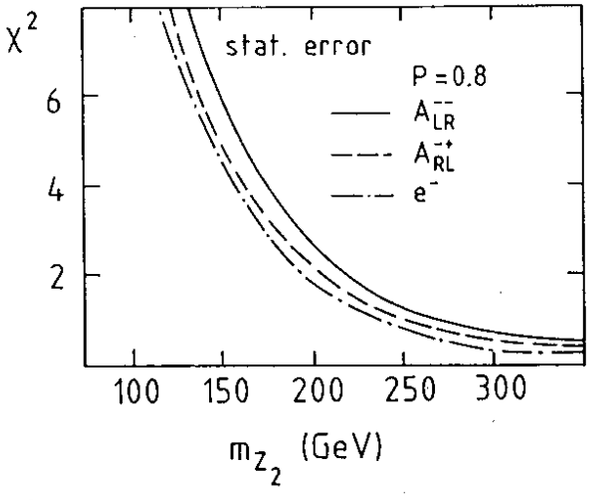

Figure 3a
The quantity $\chi^2(m_{Z_2})$ defined in eq. (43), for model A (taking $\theta = 0$) and for the most sensitive asymmetry(ies) and unpolarized cross-section. The statistical errors assumed correspond to an integrated luminosity of 125 pb^{-1} per polarized beam and 250 pb^{-1} per unpolarized beam. The degree of polarization is assumed to be 80%

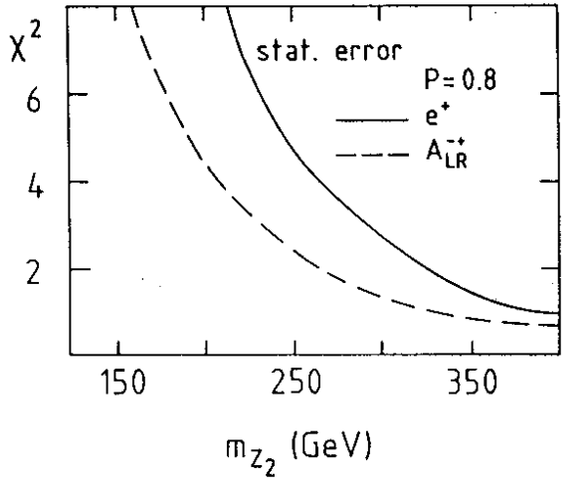

Figure 3b
Same as Fig. 3a, for model B

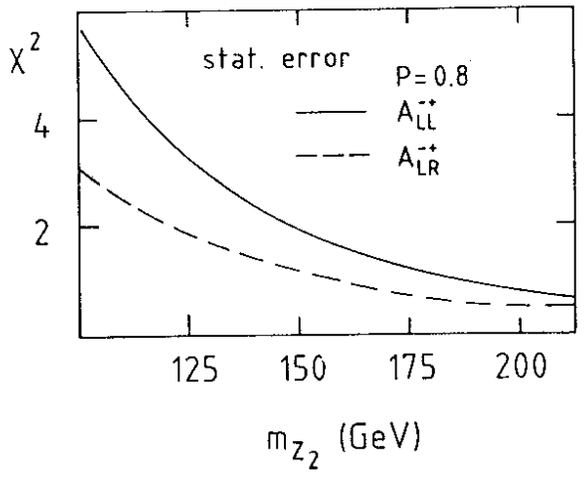

Figure 3c
Same as Fig. 3a, for model C

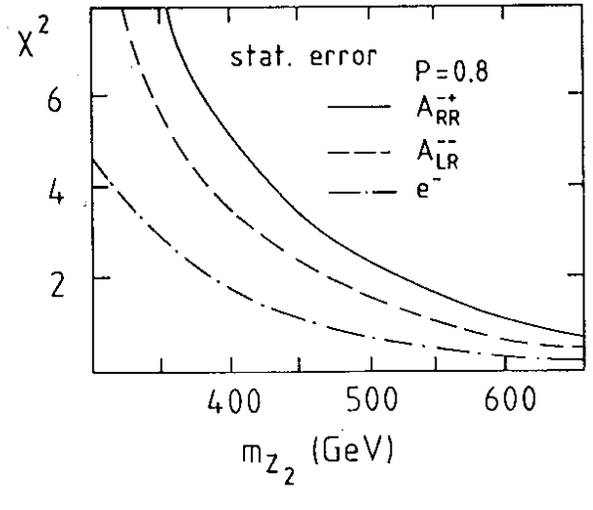

Figure 3d
Same as Fig. 3a, for the left-right symmetric model

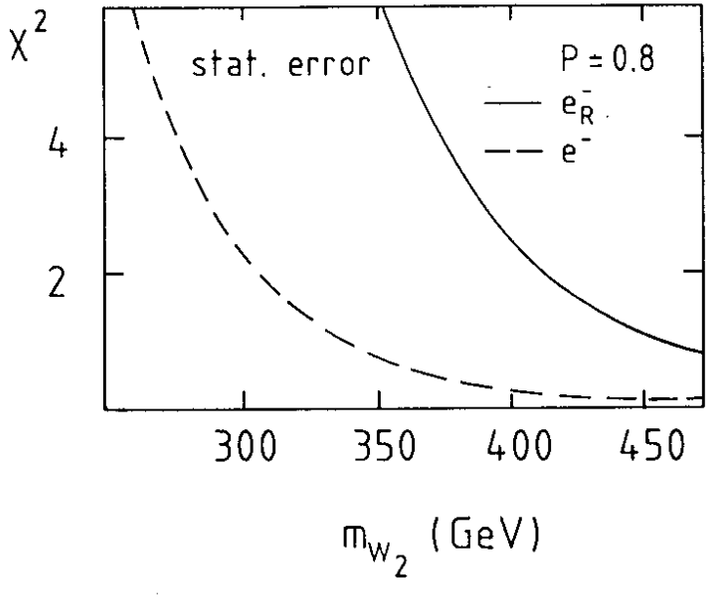

Figure 4
The quantity $\chi^2(m_{W_2})$ defined in eq. (43), in the case of a W' coupled to right-handed currents (taking $\zeta = 0$). The χ^2 obtained for the ratio of ϵ_R^- and ϵ_L^- CC cross-sections is very similar to the result for the ϵ_R^- cross-section itself. The latter is shown in comparison to the χ^2 for the unpolarized ϵ^- CC cross-section. The statistical errors assumed correspond to an integrated luminosity of 125 pb^{-1} per polarized beam and 250 pb^{-1} per unpolarized beam. The degree of polarization is assumed to be 80%